Dalton Transactions

ROYAL SOCIETY OF CHEMISTRY

PAPER

View Article Online
View Journal | View Issue

Check for updates

Cite this: *Dalton Trans.*, 2022, **51**, 11448

Titanium complexes with unsymmetrically substituted imidazolin-2-iminato ligands†

Marvin Koneczny,[a] Arife Büsra Erol,[a] Marc Mauduit,[b] Moris S. Eisen[c] and Matthias Tamm*[a]

Received 3rd June 2022,
Accepted 8th July 2022

DOI: 10.1039/d2dt01740g

rsc.li/dalton

The reaction of the unsymmetrical N-heterocyclic carbenes 1-(2,4,6-trimethylphenyl)-3-(adamantyl) imidazolin-2-ylidene (IAdMes, **1a**) and 1-(2,6-diisopropylphenyl)-3-(adamantyl)imidazolin-2-ylidene (IAdDipp, **1b**) with trimethylsilyl azide furnished the 2-(trimethylsilylimino)imidazolines **2a** ($Im^{AdMes}NSiMe_3$) and **2b** ($Im^{AdDipp}NSiMe_3$). Desilylation by stirring in methanol gave the corresponding imidazolin-2-imines **3a** ($Im^{AdMes}NH$) and **3b** ($Im^{AdDipp}NH$). **2a** and **2b** were treated with $[TiCl_4(THF)_2]$ (THF = tetrahydrofuran) and $[CpTiCl_3]$ (Cp = η^5-C_5H_5) to form the mono- and bis(imidazolin-2-iminato) titanium(IV) complexes $[(Im^{AdR}N)TiCl_3]$ (**4**, R = Mes, Dipp), $[Cp(Im^{AdR}N)TiCl_2]$ (**5**, R = Mes, Dipp), and $[(Im^{AdR}N)_2TiCl_2]$ (**6**, R = Mes, Dipp). The crystal structures of all compounds except **2b** were determined by X-ray diffraction analysis.

Introduction

Imidazolin-2-imines (Im^RNH) and their deprotonated, anionic counterparts, imidazolin-2-imides (Im^RN^-), have become important additions to the class of nitrogen donor ligands after their introduction by Kuhn and co-workers.[1,2] The widespread use of these systems was largely triggered by Tamm *et al.* through the development of a versatile synthetic protocol based on the reaction of N-heterocyclic carbenes (NHCs) of the imidazolin-2-ylidene-type with trimethylsilyl azide followed by desilylation.[3–5] The intermediate silylated imines Im^RNSiMe_3 may serve as suitable precursors for the preparation of imidazolin-2-iminato transition metal complexes, which feature short metal–nitrogen bonds owing to the ability of these ligands to act as strong 2σ-/4π-electron donors, preferably to early transition metals and/or metals in higher oxidation states.[6] Accordingly, numerous homogeneous d^0-metal (pre-) catalysts with ancillary imidazolin-2-iminato ligands have been developed, with titanium(IV) complexes of type **I** and their use in olefin polymerisation representing the most prominent application (Fig. 1).[4,7–9] Related titanium complexes with additional aryloxo,[10,11] amido,[11,12] and guanidinate ligands[13] were also reported, while imidazolidin-2-iminato-titanium complexes represent a closely related class of olefin polymerisation and oligomerisation catalysts.[14] In contrast, zirconium and hafnium imidazolin-2-iminato complexes have so far found significantly less application in homogeneous catalysis.[15] Furthermore, imidazolin-2-iminato-supported vanadium (V) imido complexes of type **II** were employed in ethylene (co-) polymerisation and ring-opening metathesis polymerisation,[16] whereas molybdenum(VI) and tungsten(VI) alkylidyne complexes of type **III** served as highly active alkyne metathesis catalysts.[17]

Very short metal–nitrogen bonds were also found in rare-earth metal imidazolin-2-iminato complexes such as **IV**,[18–20] which were employed as hydroamination and hydrosilylation catalysts.[21] Recently, the dysprosium(III) complex $[(Im^{Dipp}N)DyCl_2(THF)_3]$ was presented as a suitable single-molecule magnet.[22] Moreover, numerous actinide complexes such as the thorium(IV) and uranium(IV) complexes **V** were prepared,[23] with these and related complexes serving as highly active catalysts for ring-opening polymerisation, hydroelementation, and aldehyde disproportionation (Tishchenko) reactions.[24] Uranium(III) complexes were also reported and used for the generation of a photochemically generated terminal uranium nitride.[25]

All of the compounds shown in Fig. 1, like most of the known imidazolin-2-iminato complexes, have a symmetrical *N*,*N*-substitution pattern, whereas unsymmetrical systems are rare.[26] Recently, however, Eisen and co-workers presented unsymmetrical benzimidazolin-2-iminato ligands and their application primarily in the development of organoactinide catalysts.[27] These systems contain a combination of bulky *N*-aryl and small *N*-alkyl substituents to create more accessible,

[a]*Institut für Anorganische und Analytische Chemie, Technische Universität Braunschweig, Hagenring 30, 38106 Brauschweig, Germany. E-mail: m.tamm@tu-bs.de*
[b]*Univ Rennes, Ecole Nationale Supérieure de Chimie de Rennes, CNRS, ISCR-UMR 6226, F-35000 Rennes, France*
[c]*Schulich Faculty of Chemistry, Technion – Israel Institute of Technology, Technion City, 32000 Haifa, Israel*

†Electronic supplementary information (ESI) available: NMR spectra, crystallographic details. CCDC 2174864–2174874. For ESI and crystallographic data in CIF or other electronic format see DOI: https://doi.org/10.1039/d2dt01740g

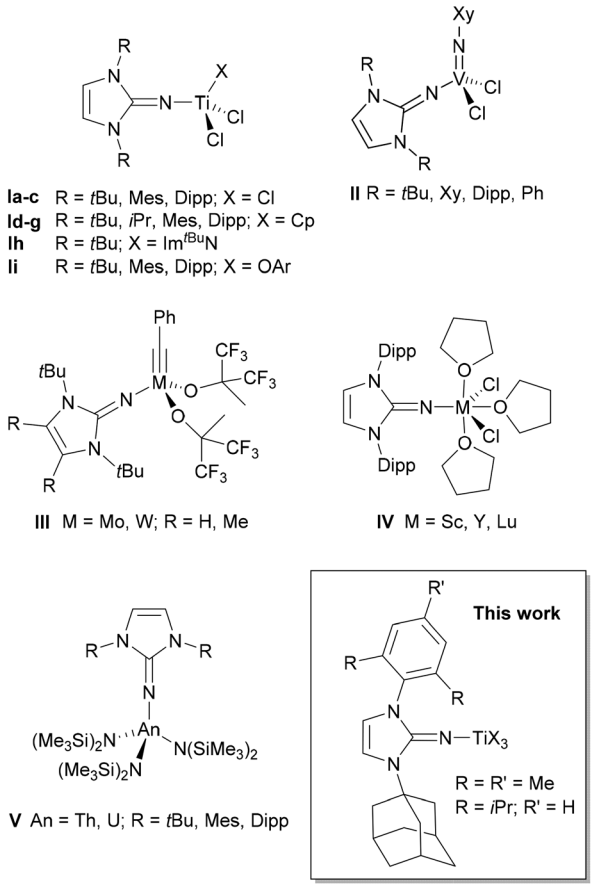

Fig. 1 Selected examples for imidazolin-2-iminato complexes. Mes = 2,4,6-trimethylphenyl, Dipp = 2,6-diisopropylphenyl, Xy = 2,6-dimethylphenyl.

sterically less encumbered catalysts. In search for unsymmetrical imidazolin-2-iminato ligands with two different, yet bulky *N*-substituents, we identified the carbenes 1-(2,4,6-trimethylphenyl)-3-(adamantyl)imidazolin-2-ylidene (IAdMes, **1a**) and 1-(2,6-diisopropylphenyl)-3-(adamantyl)imidazolin-2-ylidene (IAdDipp, **1b**), introduced by Mauduit, Baslé and co-workers,[28,29] as suitable starting materials for the synthesis of the corresponding imidazolin-2-imines. These NHC ligands have been used, for example, for the preparation of highly *Z*-selective olefin metathesis ruthenium catalysts,[30] and in principle, the corresponding imidazolin-2-iminato ligands might also pave the way to their application in asymmetric homogeneous catalysis. Accordingly, we wish to present herein the isolation and structural characterisation of the free carbenes IAdMes (**1a**) and IAdDipp (**1b**) as well as their use as starting materials for the preparation of unsymmetrical imidazolin-2-imines $Im^{AdMes}NR$ (**2a**, R = $SiMe_3$; **3a**, R = H) and $Im^{AdDipp}NR$ (**2b**, R = $SiMe_3$; **3b**, R = H). In addition, the silylated imines were used for the synthesis of a series of mono- and bis(imidazolin-2-iminato) titanium(IV) complexes to allow comparison with their well-established symmetrical congeners of type **I** (Fig. 1).

Results and discussion

Preparation and characterisation of imidazolin-2-imine ligands

Based on the unsymmetrical *N*-substituted imidazolium salts established by Mauduit and Baslé,[28,29] the corresponding free carbenes **1a** and **1b** can be generated by deprotonation with KO*t*Bu in THF (Scheme 1). Since the free NHCs were previously always generated *in situ*, full analytical data will be provided herein. The carbenes **1a** and **1b** show typical sets of signals for the protons in the 4,5-position of the heterocycle in the ^{1}H NMR spectra as doublets with chemical shifts of 6.88/6.50 ppm (**1a**) and 6.84/6.63 ppm (**1b**). Significantly deshielded ^{13}C NMR resonances at 216.1 ppm (**1a**) and 217.0 ppm (**1b**) clearly indicate the formation of the free carbenes. The 2-(trimethylsilylimino)imidazolines **2a** and **2b** were prepared by treatment of the corresponding imidazolin-2-ylidenes **1a** and **1b** with trimethylsilyl azide in boiling toluene following the established procedure.[3–5] **2a** and **2b** were isolated as pale yellow solids after bulb-to-bulb distillation of the crude brownish viscous oils and subsequent washing with or crystallisation from *n*-hexane. The product formation can be followed by ^{1}H NMR spectroscopy, as there is a clear upfield shift of the resonances of the hydrogen atoms in the 4,5-position (backbone) to 6.16/5.66 ppm (**2a**) and 6.19/5.89 ppm (**2b**), consistent with the observations for the symmetrically substituted analogues.[5] In addition, the relatively narrow multiplets observed for the distal CH_2 groups in the carbene starting materials broaden and evolve into doublets of doublets in agreement with the presence of diastereotopic hydrogen atoms. The resonances of the trimethylsilyl protons appear at 0.09 ppm (**2a**) and 0.07 ppm (**2b**). In the ^{13}C NMR spectra, the resonances for the N*C*N atoms are shifted to higher field by *ca.* −75 ppm compared to the free carbenes and are found at 141.2 ppm (**2a**) and 141.0 ppm (**2b**). Desilylation of **2a** and **2b** was accomplished by stirring their methanol solutions for short periods of time (30–120 min). The ^{1}H NMR spectra exhibit broad signals for the NH hydrogen atoms at 4.46 ppm (**3a**) and 4.38 ppm (**3b**), while the resonances of the carbene moieties remain rather unaffected in comparison with **2a** and **2b**. In contrast, a significant downfield shift of *ca.* 10 ppm can be found for the N*C*N resonances in the ^{13}C NMR spectra, resulting in chemical shifts of 153.1 ppm (**3a**) and 154.4 ppm (**3b**).

To compare the new ligands with the previously established ones,[3,5] the molecular structures of **1a**, **1b**, **2a**, **3a**, and **3b** were

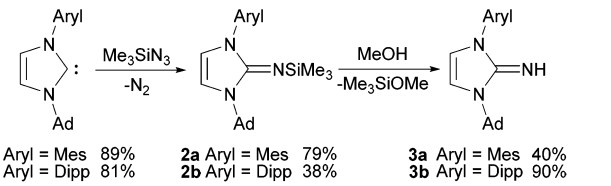

Scheme 1 Preparation of the unsymmetrical *N*-substituted imidazolin-2-imines. Mes = 2,4,6-trimethylphenyl, Dipp = 2,6-diisopropylphenyl.

Table 1 Selected bond lengths [Å] and angles [°] for compounds **1a**, **1b**, **2a**, **3a**, and **3b**

	C1–N1	N1–Si1/H1	N2–C1–N3	C1–N1–Si1
1a	1.3739(5)		102.05(3)	
	1.3651(5)			
1b	1.3709(18)		101.48(11)	
	1.3627(18)			
2a	1.2782(10)	1.6823(7)	103.99(6)	142.68(7)
3a	1.2966(14)	0.902(16)	104.55(9)	
3b	1.2891(13)	0.926(14)	104.78(8)	

established by X-ray diffraction analysis; single crystals of **2b** were not obtained due to its high solubility in *n*-hexane. Pertinent structural parameters are assembled in Table 1, and presentations of the structures are depicted in Fig. 2. **1a** and **1b** exhibit N–C–N angles of 102.05(3)° and 101.48(11)°, which are as expected significantly smaller than those reported for the imidazolium salt ([IAdMesH]Cl = 108.56(12)°)[28] and clearly indicate the formation of free carbenes. The C1–N1 bond length of 1.2782(10) Å in **2a** agrees well with the values reported for the corresponding imines $Im^{Mes}NSiMe_3$ (1.267(2) Å)[5] and $Im^{tBu}NSiMe_3$ (1.275(3) Å)[3] and falls in the range expected for C–N double bonds.[31] The trimethylsilyl (TMS) group in **2a** points towards the mesityl substituent, and accordingly, the C1–N1–Si1 angle of 142.68(7)° is similar to 147.2(1)° in $Im^{Mes}NSiMe_3$, whereas significantly larger angles of 155.4(1)° and 169.3(2)° were observed for $Im^{Dipp}NSiMe_3$ and $Im^{tBu}NSiMe_3$, respectively.[3,5] The position of hydrogen atoms in **3a** and **3b** could be freely refined, both facing the aryl group. The C1–N1 bond lengths are 1.2966(14) Å (**3a**) and 1.2891(13) Å (**3b**), which falls in the range reported for other imidazolin-2-imines,[5] *e.g.*, 1.284(2) Å in $Im^{Mes}NH$[32] and 1.289 (2) Å in $Im^{Dipp}NH$.[20]

Preparation and characterisation of titanium imidazolin-2-iminato complexes

To introduce the new unsymmetrically *N*-substituted imidazolin-2-imines to transition metal chemistry, a series of titanium complexes was prepared, following the approach established since the earliest reports in the field.[2–4] Thus, the silylated imines **2a** and **2b** were treated with titanium chloride precursors in toluene solution to afford the corresponding titanium complexes **4–6**, with Me_3SiCl formation as the driving force of the reaction (Scheme 2). Treatment with $[TiCl_4(THF)_2]$ or $[CpTiCl_3]$ (Cp = η^5-cyclopentadienyl) at room temperature gave the mono(imidazolin-2-iminato) complexes **4a**/**4b** or **5a**/**5b** as orange-red crystalline solids after stirring for 16 h, followed by evaporation and washing with *n*-hexane. The preparation of the bis(imidazolin-2-iminato) complexes **6a**/**6b** required more forcing conditions, and the reaction of $[TiCl_4(THF)_2]$ with two equivalents of **2a**/**2b** in toluene at 100 °C afforded **6a**/**6b** as orange crystalline solids after similar work-up. The significantly harsher reaction conditions required for the introduction of the second ligand point to the possibility of sequential introduction of two different imidazolin-2-iminato ligands in the future. The ^1H and ^{13}C NMR spectra of the complexes **4–6** are very similar, with little influence of metal coordination on the NHC signals. For the Cp complexes **5a**/**5b**, the signals at 6.05/5.90 ppm and 114.8/115.3 ppm can be assigned to the

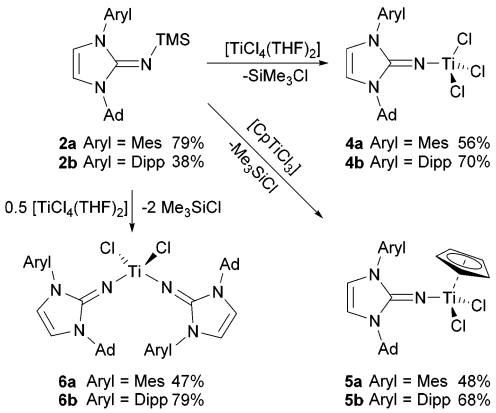

Scheme 2 Preparation of titanium complexes bearing $Im^{AdAryl}N$ ligands. Ad = adamantly, Mes = 2,4,6-trimethylphenyl, Dipp = 2,6-diisopropylphenyl.

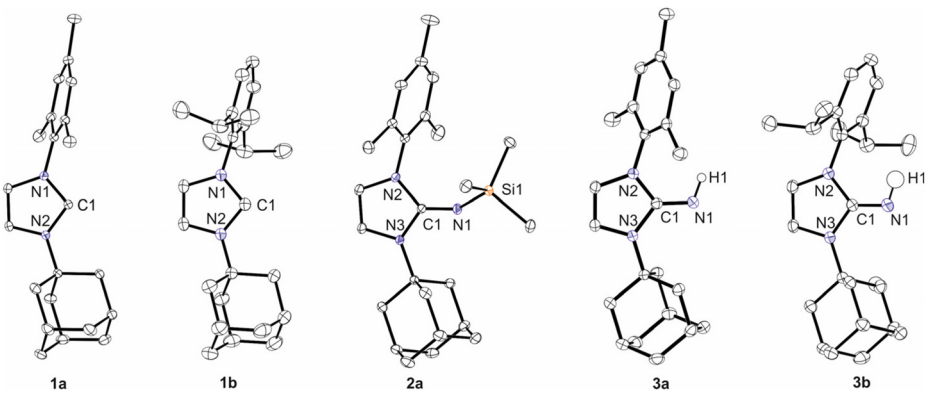

Fig. 2 Molecular structures of **1a**, **1b**, **2a**, **3a** and **3b** with thermal displacement parameters drawn at 50% probability. Hydrogen atoms, except H1, are omitted for clarity. For further information on the X-ray diffraction analysis please refer to the ESI.†

C_5H_5 hydrogen and carbon atoms, respectively. It should be noted that the room-temperature NMR spectra of the bis(imidazolin-2-iminato) complexes **6a** and **6b** reveal dynamic behaviour in solution, since only one set of signals for the NHC fragment is observed in each case. Therefore, a variable-temperature ^{1}H NMR study was conducted for **6b**, which led to a splitting of the isopropyl signals below a coalescence temperature of about −40 °C (see ESI†). This evolves the original two doublets and one septet (or quartet–quartet) into four doublets and two septets, which can be attributed to the presence of diastereotopic isopropyl groups in either C_2- or C_s-symmetric conformers (*vide infra*).

The new complexes **4–6** were additionally characterised by X-ray diffraction analysis, and the resulting molecular structures are presented in Fig. 3. Pertinent structural data are assembled in Table 2. The titanium atoms in the $TiCl_3$ complexes **4a**/**4b** exhibit only slightly distorted tetrahedral geometries and short Ti–N distances of 1.7347(5) Å (**4a**) and 1.7316(17) Å (**4b**), which are in good agreement with the values reported for [(Im^{Mes}N)TiCl$_3$] and [(Im^{Dipp}N)TiCl$_3$] and indicate strong π-donation towards the metal atom.[9] The Ti1–N1–C1 angles are 162.58(5)° in **4a** and 173.04(16)° in **4b**, with the former deviating significantly from linearity, presumably due to different steric demands of the mesityl and adamantyl substituents. For the cyclopentadienyl complexes **5**, slightly longer Ti1–N1 bond lengths of 1.7758(16) Å (**5a**) and 1.7760(5) Å (**5b**) together with large Ti1–N1–C1 angles of 170.26(14)° (**5a**) and 170.86(5)° (**5b**) are found, which agrees well with the structural characteristics established for related systems, *e.g.*, 1.765(3) Å and 170.7(2)° in [Cp(Im^{tBu}N)TiCl$_2$][3] as well as 1.778(2) Å and 175.8(1)° in [Cp(Im^{Dipp}N)TiCl$_2$].[4] The bis(imidazolin-2-iminato) complexes **6a** and **6b** exhibit the longest Ti–N distances of complexes **4–6**, namely 1.7951(15)/1.7867(16) Å (**6a**) and 1.7994(18)/1.8067(18) Å (**6b**), which is slightly longer compared to 1.788(2)/1.790(2) Å in [(Im^{tBu}N)$_2$TiCl$_2$].[8] The Ti–N–C

Table 2 Selected bond lengths [Å] and angles [°] for compounds **4–6**. For complexes **6** the respective values of C23–N4/Tl1–N4/Ti1–N4–C23/N5–C23–N6 are given in the second row

	C1–N1	Ti1–N1	Ti1–N1–C1	N2–C1–N3
4a	1.3265(7)	1.7347(5)	162.58(5)	107.41(4)
4b	1.330(3)	1.7316(17)	173.04(16)	106.89(17)
5a	1.319(2)	1.7758(16)	170.26(14)	105.99(15)
5b	1.3189(8)	1.7760(5)	170.86(5)	106.13(5)
6a	1.304(2)	1.7951(15)	166.51(13)	105.89(14)
	1.302(2)	1.7867(16)	166.94(13)	105.69(15)
6b	1.304(3)	1.7994(18)	167.14(17)	105.69(18)
	1.302(3)	1.8067(18)	167.64(17)	105.24(18)

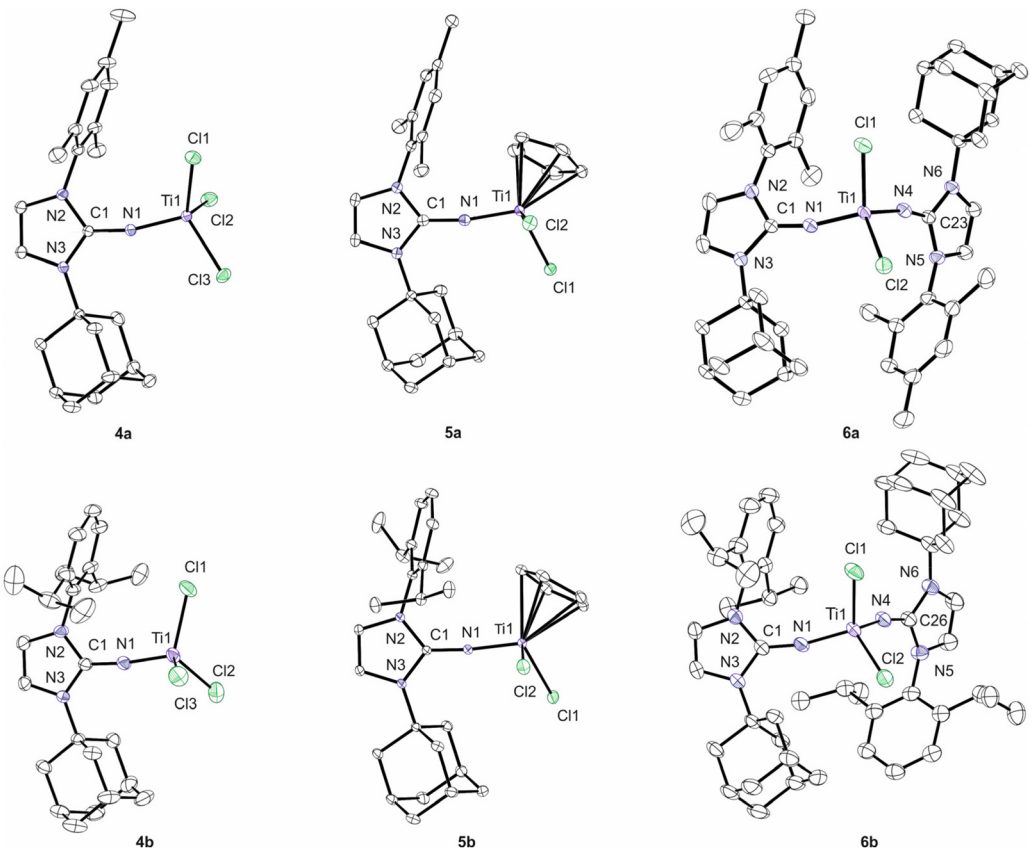

Fig. 3 Molecular structures of **4a**, **4b**·CH_2Cl_2·Solv., **5a**, **5b**, **6a**·0.5CH_2Cl_2 and **6b**·CH_2Cl_2 with thermal displacement parameters drawn at 50% probability. Hydrogen atoms and co-crystallised solvent molecules are omitted for clarity. The molecular structure of **4b** contains disordered solvent molecules along a tube-shaped solvent accessible void. For further information on the X-ray diffraction analysis please refer to the ESI.†

angles of 166.51(13)°/166.94(13)° (**6a**) and 167.14(17)°/167.64 (17)° (**6b**) indicate slightly stronger bending, which can be ascribed to the asymmetric *N*,*N*-substitution pattern of the imidazolin-2-iminato ligands. Above all, the latter adopt C_2-symmetric orientations in the solid state with the aryl and adamantyl substituents of two the ligands facing in opposite directions. Accordingly, it is reasonable to assume that these chiral conformations also exist in solution, albeit only at low temperatures (*vide supra*).

Conclusions

Imidazolin-2-imines with an unsymmetrical aryl-adamantyl substitution pattern were prepared from the free N-heterocyclic carbenes IAdMes (**1a**) and IAdDipp (**1b**). The reactions of the silylated imines $Im^{AdMes}NSiMe_3$ (**2a**) and $Im^{AdDipp}NSiMe_3$ (**2b**) with $[TiCl_4(THF)_2]$ and $[CpTiCl_3]$ provided a series of mono- and bis(imidazolin-2-iminato) titanium complexes **4–6** with release of trimethylsilyl chloride. All titanium complexes feature short metal–nitrogen bonds and large Ti–N–C angles (162°–173°), confirming the ability of these systems to act as electron-rich imido-type N-donor ligands. These complexes could serve as efficient olefin polymerisation pre-catalysts, with the asymmetry introduced by the unsymmetrical substitution pattern possibly enabling their application in stereospecific olefin polymerisation.[33] This aspect will be under investigation in due course. In general, these ligands enrich the portfolio of available imidazolin-2-imine systems, which are not only widely used ligands in transition metal,[6] rare earth metal,[19] and actinide chemistry,[23] but have also found considerable attention in main group element chemistry.[34]

Experimental details

Materials and methods

All operations with air- and moisture-sensitive compounds were performed in a glove box under a dry argon atmosphere (MBraun GmbH, MB20G) or on a vacuum line using Schlenk techniques. Solvents were either purified *via* standard methods[35] or obtained by purification with an Mbraun SPS and subsequently stored over Molecular Sieves (3–4 Å). Deuterated solvents were distilled from Na/K or CaH_2, and degassed prior to use. The ^1H and $^{13}C\{^1H\}$ NMR spectra were recorded on Bruker AVII300, Bruker AVIIHD400, Bruker AVIIIHD500 and Bruker AVII600 spectrometers at room temperature. ^1H and $^{13}C\{^1H\}$ NMR spectra were referenced against the (residual) solvent signals.[36] Chemical shifts are reported in ppm (parts per million). Coupling constants (*J*) are reported in Hertz (Hz), and splitting patterns are indicated as s (singlet), d (doublet), t (triplet), q (quartet), m (multiplet), sept (septet) and br (broad). NMR assignments were made using additional 2D NMR experiments. Elemental analysis was carried out with a Vario Micro Cube System. Unless otherwise indicated, all starting materials were obtained from Sigma-Aldrich, ABRC, TCI, Acros or Fluka and were purified if necessary. [IAdMesH]Cl[28,29] and [IAdDippH]Cl[28,29] were prepared according to literature procedures.

Synthetic procedures

IAdMes (1a). A suspension of KO*t*Bu (1.99 g, 22.3 mmol, 1.1 eq.) in 10 mL THF was added to a solution of [IAdMesH]Cl (5.76 g, 16.1 mmol, 1 eq.) in 100 mL THF. The mixture was stirred for 3 h at room temperature, and the solvent was subsequently removed under high vacuum. The residue was then dissolved in 80 mL of hot toluene and filtered through Celite®, and the frit was washed two times with *ca.* 10 mL of hot toluene. After removal of all volatiles under high vacuum an off-white solid could be obtained. The solid was layered with 20 mL of *n*-hexane, the suspension was stirred for 5 minutes at 60 °C and then placed to cool in an ice bath. The supernatant solution was removed *via* a syringe and the remaining solvent then evaporated under high vacuum to obtain product **1a** as colorless crystalline powder (4.58 g, 14.3 mmol, 89%).

^1H NMR (500 MHz, C_6D_6): δ = 6.88 (d, $^3J_{HH}$ = 1.6 Hz, 1H, C*H*-backbone), 6.83–6.79 (m, 2H, *m*-Mes), 6.50 (d, $^3J_{HH}$ = 1.8 Hz, 1H, C*H*-backbone), 2.28 (d, $^3J_{HH}$ = 2.8 Hz, 6H, CH_2-Ad), 2.15 (s, 3H, *p*-CH_3), 2.13 (s, 6H, *o*-CH_3), 2.02 (br. s, 3H, C*H*-Ad), 1.66–1.52 (br. m, 6H, CH_2-Ad).

^{13}C NMR (126 MHz, C_6D_6): δ = 216.1 (s, N–*C*–N), 140.0 (s, i-Mes), 136.9 (s, *p*-Mes), 135.5 (s, *o*-Mes), 129.0 (s, *m*-Mes), 119.4 (s, *C*H-backbone), 114.8 (s, *C*H-backbone), 56.2 (s, *C*q-Ad), 44.9 (s, *C*H_2-Ad), 36.6 (s, *C*H_2-Ad), 30.3 (s, *C*H-Ad), 21.0 (s, *p*-*C*H_3), 18.2 (s, *o*-*C*H_3).

EA (%) calc. for $C_{22}H_{28}N_2$ (320 g mol^{-1}): C 82.45, H 8.81, N 8.74; found: C 82.57, H 8.893, N 8.74.

IAdDipp (1b). A suspension of KO*t*Bu (5.22 g, 46.5 mmol, 1.1 eq.) in 25 mL THF was added to a solution of [IAdDippH]Cl (16.97 g, 42.3 mmol, 1 eq.) in 150 mL THF. The mixture was stirred for 40 min at room temperature and the solvent was subsequently removed under high vacuum. The residue was dissolved in 350 mL of hot toluene and filtered through Celite®, and the frit was washed two times with *ca.* 10 mL of hot toluene. After removal of all volatiles under high vacuum an off-white solid could be obtained. The solid was then layered with 30 mL of *n*-hexane, the suspension was stirred for 5 minutes at 60 °C and placed to cool in an ice bath. The supernatant solution was removed *via* a syringe and the remaining solvent then evaporated under high vacuum to obtain product **1b** as colorless crystalline powder (12.46 g, 34.4 mmol, 81%).

^1H NMR (300 MHz, C_6D_6): δ = 7.29–7.22 (m, 1H, *p*-Dipp), 7.16–7.11 (m, 2H, *m*-Dipp), 6.84 (d, $^3J_{HH}$ = 1.6 Hz, 1H, CH-backbone), 6.63 (d, $^3J_{HH}$ = 1.6 Hz, 1H, CH-backbone), 2.84 (sept., $^3J_{HH}$ = 7.0 Hz, 2H, C*H*(CH_3)$_2$), 2.22 (m, 6H, CH_2-Ad), 1.97 (br. s, 3H, C*H*-Ad), 1.54 (br. s, 6H, CH_2-Ad), 1.22 (d, $^3J_{HH}$ = 6.8 Hz, 6H, CH(CH_3)$_2$), 1.11 (d, $^3J_{HH}$ = 6.8 Hz, 6H, CH(CH_3)$_2$).

^{13}C NMR (75 MHz, C_6D_6): δ = 217.0 (s, N*C*N), 146.4 (s, *o*-Dipp), 139.9 (s, i-Dipp), 128.7 (s, *p*-Dipp), 123.6 (s, *m*-Dipp),

120.6 (s, *C*H-backbone), 114.6 (s, *C*H-backbone), 56.2 (s, *C*q-Ad), 44.8 (s, CH_2-Ad), 36.6 (s, CH_2-Ad), 30.3 (s, *C*H-Ad), 28.6 (s, $CH(CH_3)_2$), 24.6 (s, $CH(CH_3)_2$), 24.0 (s, $CH(CH_3)_2$).

EA (%) calc. for $C_{25}H_{34}N_2$ (363 g mol^{-1}): C 82.82, H 9.45, N 7.73; found: C 82.67, H 9.481, N 7.21.

Im^{AdMes}NSiMe$_3$ (2a). A solution of carbene **1a** (4.58 g, 14.3 mmol, 1 eq.) in 70 mL toluene was slowly treated with trimethylsilylazide (2.64 mL, 20 mmol, 1.4 eq.) at room temperature. The mixture was heated to reflux for 72 h, during which the formation of an off-white solid could be observed. After cooling to room temperature, the suspension was filtered, and all volatiles were removed under high vacuum. The resulting yellow viscous residue was purified by bulb-to-bulb distillation at high vacuum (5×10^{-2} mbar) with the aid of two heat guns. The obtained residue could be crystallised from hot *n*-hexane to obtain product **2a** as a light yellow crystalline solid (4.60 g, 11.3 mmol, 79%). For further purification the product could be sublimed at 1×10^{-3} mbar and 165 °C.

^{1}H NMR (500 MHz, C_6D_6): δ = 6.79–6.77 (m, 2H, *m*-Mes), 6.16 (d, $^3J_{HH}$ = 3.0 Hz, 1H, C*H*-backbone), 5.66 (d, $^3J_{HH}$ = 3.1 Hz, 1H, CH-backbone), 2.36 (d, $^3J_{HH}$ = 2.7 Hz, 6H, CH_2-Ad), 2.13 (s, 6H, *o*-CH_3), 2.10 (s, 3H, *p*-CH_3), 2.03 (br. s., 3H, C*H*-Ad), 1.71–1.55 (br. m, 6H, CH_2-Ad), 0.09 (s, 9H, Si(CH_3)$_3$).

^{13}C NMR (126 MHz, C_6D_6): δ = 141.2 (s, N*C*N), 138.1 (s, *p*-Mes), 137.7 (s, *o*-Mes), 134.8 (s, i-Mes), 129.3 (s, *m*-Mes), 110.2 (s, *C*H-backbone), 109.3 (s, *C*H-backbone), 55.7 (s, *C*q-Ad), 39.7 (s, CH_2-Ad), 36.7 (s, CH_2-Ad), 30.2 (s, C*H*-Ad), 21.1 (s, *p*-*C*H_3), 18.3 (s, *o*-*C*H_3), 3.5 (s, Si(*C*H_3)$_3$).

EA (%) calc. for $C_{25}H_{37}N_3Si$ (408 g mol^{-1}): C 73.66, H 9.15, N 10.31; found: C 73.95, H 9.032, N 10.00.

Im^{AdDipp}NSiMe$_3$ (2b). A solution of carbene **1b** (4.00 g, 11.0 mmol, 1 eq.) in 100 mL toluene was slowly treated with trimethylsilylazide (2.18 mL, 16.5 mmol, 1.5 eq.) at room temperature. The mixture was heated to reflux for 72 h, during which the formation of an off-white solid could be observed. After cooling to room temperature, the suspension was filtered and all volatiles were removed under high vacuum. The resulting yellow viscous residue was purified by bulb-to-bulb distillation at high vacuum (5×10^{-2} mbar) with the aid of two heat guns. The obtained residue was washed with small amounts of *n*-hexane to obtain product **2b** as a light-yellow solid (1.91 g, 4.2 mmol, 38%).

^{1}H NMR (400 MHz, C_6D_6): δ = 7.24–7.19 (m, 1H, *p*-Dipp), 7.13–7.10 (m, 2H, *m*-Dipp), 6.19 (d, $^3J_{HH}$ = 3 Hz, 1H, C*H*-backbone), 5.89 (d, $^3J_{HH}$ = 3 Hz, 1H, C*H*-backbone), 3.01 (sept, $^3J_{HH}$ = 6.89 Hz, 2H, C*H*(CH_3)$_2$), 2.33 (d, $^3J_{HH}$ = 2.7 Hz, 6H, CH_2-Ad), 2.01 (br. s, 3H, C*H*-Ad), 1.69–1.53 (br. m., 6H, CH_2-Ad), 1.33 (d, $^3J_{HH}$ = 6.9 Hz, 6H, CH(CH_3)$_2$), 1.11 (d, $^3J_{HH}$ = 6.9 Hz, 6H, CH(CH_3)$_2$), 0.07 (s, 9H, Si(CH_3)$_3$).

^{13}C NMR (100 MHz, C_6D_6): δ = 148.3 (s, *o*-Dipp), 141.0 (N*C*N), 135.5 (s, i-Dipp), 129.5 (s, *p*-Dipp), 124.2 (s, *m*-Dipp), 112.3 (s, *C*H-backbone), 108.7 (s, *C*H-backbone), 55.7 (s, *C*q-Ad), 39.8 (s, CH_2-Ad), 36.7 (s, CH_2-Ad), 30.2 (s, *C*H-Ad), 28.7 (s, *C*H(CH_3)$_2$), 25.0 (s, CH(*C*H$_3$)$_2$), 23.1 (s, CH(*C*H$_3$)$_2$), 3.5 (s, Si(*C*H_3)$_3$).

EA (%) calc. for $C_{28}H_{43}N_3Si$ (450 g mol^{-1}): C 74.78, H 9.64, N 9.34, found: C 75.27, H 9.481, N 9.29.

Im^{AdMes}NH (3a). Imine **2a** (3.00 g, 7.36 mmol, 1 eq.) was treated with 40 mL methanol and the resulting solution was stirred for 2 h at room temperature. The solvent was then removed under high vacuum and the resulting off-white solid could be crystallised from hot *n*-hexane. The crystalline solid was washed three times with small amounts of *n*-hexane and residual solvent was removed under high vacuum. Subsequent sublimation at 1×10^{-3} mbar and 130–140 °C gave compound **3a** as a colorless powder (1.00 g, 2.98 mmol, 40%).

^{1}H NMR (400 MHz, C_6D_6): δ = 6.71 (m, 2H, *m*-Mes), 6.16 (d, $^3J_{HH}$ = 2.9 Hz, 1H, C*H*-backbone), 5.66 (d, $^3J_{HH}$ = 2.8 Hz, 1H, C*H*-backbone), 4.46 (s, 1H, N*H*), 2.53 (br.s, 6H, CH_2-Ad), 2.09 (s, 6H, *o*-CH_3), 2.07 (s, 3H, *p*-CH_3), 2.03 (br. s., 3H, C*H*-Ad),1.72–1.52 (br. m, 6H, CH_2-Ad).

^{13}C NMR (100 MHz, C_6D_6): δ = 153.1 (s, N*C*N), 138.2 (s, *p*-Mes), 138.0 (s, *o*-Mes), 132.9 (s, i-Mes), 129.7 (s, *m*-Mes), 109.9 (s, *C*H-backbone), 109.4 (s, *C*H-backbone), 55.9 (s, *C*q-Ad), 39.7 (s, CH_2-Ad), 36.7 (s, CH_2-Ad), 30.2 (s, *C*H-Ad), 21.0 (s, *p*-*C*H_3), 18.0 (s, *o*-*C*H_3).

EA (%) calc. for $C_{22}H_{29}N_3$ (336 g mol^{-1}): C 78.76, H 8.71, N 12.53; found: C 78.94, H 8.774, N 12.46.

Im^{AdDipp}NH (3b). Imine **2b** (0.40 g, 0.88 mmol, 1 eq.) was treated with 12 mL methanol and the resulting solution was stirred for 30 min at room temperature. The solvent volume was reduced to *ca.* 1/3 under high vacuum and 5 mL *n*-hexane were added to the solution. After stirring for an additional 30 min the volatiles were removed under high vacuum. The resulting slightly yellow solid was purified by sublimation at 2 $\times 10^{-3}$ mbar and 140 °C to yield compound **3b** as a colorless powder (0.30 g, 0.79 mmol, 90%). Alternatively, the product could be purified by crystallisation from hot *n*-hexane.

^{1}H NMR (400 MHz, C_6D_6): δ = 7.23–7.18 (m, 1H, *p*-Dipp), 7.12–7.08 (m, 2H, *m*-Dipp), 6.19 (d, $^3J_{HH}$ = 2.8 Hz, 1H, C*H*-backbone), 5.82 (d, $^3J_{HH}$ = 2.8 Hz, 1H, C*H*-backbone), 4.38 (br. s, 1H, N*H*), 3.04 (sept, $^3J_{HH}$ = 6.9 Hz, 2H, C*H*(CH_3)$_2$), 2.51 (br. s, 6H, CH_2-Ad), 2.01 (br. s, 3H, C*H*-Ad), 1.70–1.49 (br. m, 6H, CH_2-Ad), 1.23 (d, $^3J_{HH}$ = 6.9 Hz, 6H, CH(CH_3)$_2$), 1.12 (d, $^3J_{HH}$ = 6.9 Hz, 6H, CH(CH_3)$_2$).

^{13}C NMR (100 MHz, C_6D_6): δ = 154.4 (s, N*C*N), 149.3 (s, *o*-Dipp), 133.0 (s, i-Dipp), 129.9 (s, *p*-Dipp), 124.6 (s, *m*-Dipp), 111.4 (s, *C*H-backbone), 109.3 (s, *C*H-backbone), 55.9 (s, *C*q-Ad), 39.7 (s, CH_2-Ad), 36.7 (s, CH_2-Ad), 30.2 (s, *C*H-Ad), 28.8 (s, *C*H(CH_3)$_2$), 24.3 (s, CH(*C*H$_3$)$_2$), 23.9 (s, CH(*C*H$_3$)$_2$).

EA (%) calc. for $C_{25}H_{35}N_3$ (378 g mol^{-1}): C 79.53, H 9.34, N 11.13, found: C 79.66, H 9.353, N 10.48.

[(Im^{AdMes}N)TiCl$_3$] (4a). A solution of imine **2a** (100 mg, 0.25 mmol, 1 eq.) in 8 mL toluene was added to a solution of [$TiCl_4$(THF)$_2$] (82 mg, 0.25 mmol, 1 eq.) in 8 mL toluene. The yellow reaction mixture was stirred for 16 h at room temperature upon which a color change to orange could be observed. The solvent was removed under high vacuum, and the residue was washed with 3 × 3 mL *n*-hexane. After crystallisation from CH_2Cl_2/*n*-hexane the product **4a** was obtained as a red crystalline powder (68 mg, 0.14 mmol, 56%).

^{1}H NMR (500 MHz, $CDCl_3$): δ = 7.02–7.00 (m, 2H, *m*-Mes), 6.75 (d, $^3J_{HH}$ = 2.5 Hz, 1H, C*H*-backbone), 6.45 (d, $^3J_{HH}$ = 2.4

Hz, 1H, C*H*-backbone), 2.48 (br. d, $^3J_{HH}$ = 2.7 Hz, 6H, CH_2-Ad), 2.34 (s, 3H, *p*-CH_3), 2.32 (br. s, 3H, C*H*-Ad), 2.13 (s, 6H, *o*-CH_3), 1.94–1.75 (br. m, 6H, CH_2-Ad).

^{13}C NMR (126 MHz, $CDCl_3$): δ = 142.9 (s, N*C*N), 140.6 (s, *p*-Mes), 136.3 (s, *o*-Mes), 130.9 (s, i-Mes), 129.6 (s, *m*-Mes), 115.0 (s, *C*H-backbone), 110.4 (s, *C*H-backbone), 60.7 (s, *C*q-Ad), 41.0 (s, *C*H_2-Ad), 35.7 (s, *C*H_2-Ad), 29.9 (s, *C*H-Ad), 21.3 (s, *p*-*C*H_3), 17.8 (s, *o*-*C*H_3).

EA (%) calc. for $C_{22}H_{28}Cl_3N_3Ti$ (489 g mol^{-1}): C 54.07, H 5.78, N 8.60; found: C 54.04, H 6.180, N 8.20.

[(Im^{AdDipp}N)TiCl$_3$] (4b). A solution of imine **2b** (150 mg, 0.33 mmol, 1 eq.) in 10 mL toluene was added to a solution of [$TiCl_4(THF)_2$] (111 mg, 0.33 mmol, 1 eq.) in 15 mL toluene. The yellow reaction mixture was stirred for 16 h at room temperature upon which a color change to orange could be observed. The solvent was removed under high vacuum, and the residue was washed with 3 × 3 mL *n*-hexane. Subsequent removal of all volatiles under high vacuum yielded the product **4b** as an orange-red powder (120 mg, 0.23 mmol, 70%).

^{1}H NMR (600 MHz, $CDCl_3$): δ = 7.52–7.48 (m, 1H, *p*-Dipp), 7.33–7.31 (m, 2H, *m*-Dipp), 6.77 (d, $^3J_{HH}$ = 2.5 Hz, 1H, C*H*-backbone), 6.48 (d, $^3J_{HH}$ = 2.5 Hz, 1H, C*H*-backbone), 2.53 (d, $^3J_{HH}$ = 2.6 Hz, 6H, CH_2-Ad), 2.47 (sept, $^3J_{HH}$ = 6.9 Hz, 2H, C*H*(CH_3)$_2$), 2.34 (br. s, 3H, C*H*-Ad), 1.91–1.75 (br. m, 6H, CH_2-Ad), 1.37 (d, $^3J_{HH}$ = 6.8 Hz, 6H, CH(CH_3)$_2$), 1.12 (d, $^3J_{HH}$ = 6.9 Hz, 6H, CH(CH_3)$_2$).

^{13}C NMR (151 MHz, $CDCl_3$): δ = 146.4 (s, *o*-Dipp), 143.5 (s, N*C*N), 131.3 (s, *p*-Dipp), 130.8 (s, i-Dipp), 124.8 (s, *m*-Dipp), 115.8 (s, *C*H-backbone), 110.2 (s, *C*H-backbone), 60.9 (s, *C*q-Ad), 41.2 (s, *C*H_2-Ad), 35.8 (s, *C*H_2-Ad), 29.9 (s, *C*H-Ad), 29.1 (s, *C*H(CH_3)$_2$), 25.0 (s, CH(*C*H_3)$_2$), 23.3 (s, CH(*C*H_3)$_2$).

EA (%) calc. for $C_{25}H_{34}Cl_3N_3Ti$ (531 g mol^{-1}): C 56.57, H 6.46, N 7.92, found: C 56.24, H 6.585, N 7.42.

[Cp(Im^{AdMes}N)TiCl$_2$] (5a). A solution of imine **2a** (50 mg, 0.12 mmol, 1 eq.) in 1 mL toluene was added to a solution of [$CpTiCl_3$] (27 mg, 0.12 mmol, 1 eq.) in 1 mL toluene. The reaction mixture was stirred for 16 h at room temperature upon which a color change to orange could be observed. The solvent was removed under high vacuum, and the residue was washed with *n*-hexane. Subsequent removal of all volatiles under high vacuum yielded the product as an orange-red powder (31 mg, 0.06 mmol, 48%).

^{1}H NMR (600 MHz, C_6D_6): δ = 6.80–6.78 (m, 2H, *m*-Mes), 6.05 (s, 5H, Cp), 5.87 (d, $^3J_{HH}$ = 2.7 Hz, 1H, C*H*-backbone), 5.38 (d, $^3J_{HH}$ = 2.5 Hz, 1H, C*H*-backbone), 2.21 (br. d, $^3J_{HH}$ = 2.7 Hz, 6H, CH_2-Ad), 2.10 (s, 6H, *o*-CH_3), 2.08 (s, 3H, *p*-CH_3), 2.06 (br. s, 3H, C*H*-Ad), 1.91–1.50 (br. m, 6H, CH_2-Ad).

^{13}C NMR (151 MHz, C_6D_6): δ = 144.4 (s, N*C*N), 139.8 (s, *p*-Mes), 136.8 (s, *o*-Mes), 132.7 (s, i-Mes), 129.6 (s, *m*-Mes), 114.8 (s, Cp), 113.7 (s, *C*H-backbone), 109.8 (s, *C*H-backbone), 59.4 (s, *C*q-Ad), 40.5 (s, *C*H_2-Ad), 35.8 (s, *C*H_2-Ad), 30.2 (s, *C*H-Ad), 21.0 (s, *p*-*C*H_3), 18.2 (s, *o*-*C*H_3).

EA (%) calc. for $C_{27}H_{33}Cl_2N_3Ti$ (518 g mol^{-1}): C 62.56, H 6.42, N 8.11; found: C 62.19, H 6.019, N 7.87.

[Cp(Im^{AdDipp}N)TiCl$_2$] (5b). A solution of imine **2b** (100 mg, 0.22 mmol, 1 eq.) in 10 mL toluene was added to a solution of [$CpTiCl_3$] (49 mg, 0.22 mmol, 1 eq.) in 10 mL toluene. The reaction mixture was stirred for 16 h at room temperature upon which a color change could be observed. The solvent was removed under high vacuum, and the residue was crystallised from CH_2Cl_2/*n*-hexane. Removal of all volatiles under high vacuum yielded the product as an orange powder (86 mg, 0.15 mmol, 68%).

^{1}H NMR (500 MHz, $CDCl_3$): δ = 7.57–7.53 (m, 1H, *p*-Dipp), 7.41–7.39 (m, 2H, *m*-Dipp), 6.69 (d, $^3J_{HH}$ = 2.7 Hz, 1H, C*H*-backbone), 6.35 (d, $^3J_{HH}$ = 2.7 Hz, 1H, C*H*-backbone), 5.90 (s, 5H, Cp), 2.67 (sept, $^3J_{HH}$ = 6.9 Hz, 2H, C*H*(CH_3)$_2$), 2.49 (d, $^3J_{HH}$ = 2.7 Hz, 6H, CH_2-Ad), 2.27 (br. s, 3H, C*H*-Ad), 1.98–1.68 (br. m, 6H, CH_2-Ad), 1.40 (d, $^3J_{HH}$ = 6.8 Hz, 6H, CH(CH_3)$_2$), 1.10 (d, $^3J_{HH}$ = 6.9 Hz, 6H, CH(CH_3)$_2$).

^{13}C NMR (126 MHz, $CDCl_3$): δ = 147.3 (s, *o*-Dipp), 144.0 (s, N*C*N), 132.8 (s, i-Dipp), 131.1 (s, *p*-Dipp), 124.7 (s, *m*-Dipp), 115.7 (s, *C*H-backbone), 115.3 (s, Cp), 109.7 (s, *C*H-backbone), 60.0 (s, *C*q-Ad), 40.9 (s, *C*H_2-Ad), 35.8 (s, *C*H_2-Ad), 30.0 (s, *C*H-Ad), 28.9 (s, CH(*C*H_3)$_2$), 25.3 (s, CH(*C*H_3)$_2$), 23.0 (s, CH(*C*H_3)$_2$).

EA (%) calc. for $C_{30}H_{39}Cl_2N_3Ti$ (560 g mol^{-1}): C 64.30, H 7.01, N 7.50; found: C 63.85, H 7.032, N 7.14.

[(Im^{AdMes}N)$_2$TiCl$_2$] (6a). A solution of imine **2a** (1.16 g, 2.85 mmol, 2.2 eq.) in 10 mL toluene was added to a solution of [$TiCl_4(THF)_2$] (0.43 g, 1.29 mmol, 1 eq.) in 15 mL toluene. The yellow reaction mixture was stirred for 16 h at 100 °C upon which the formation of an orange solid could be observed. The suspension was cooled to room temperature, the solid was separated by filtration and then washed several times with small amounts of toluene. The residue was crystallised from CH_2Cl_2/*n*-hexane to obtain 0.36 g of product **6a**. Further crystals were obtained by cooling the mother liquor to −40 °C (0.12 g). The combined crystal fractions were dried under high vacuum yielding the product as an orange crystalline powder (0.48 g, 0.61 mmol, 47%).

^{1}H NMR (500 MHz, $CDCl_3$): δ = 6.87–6.84 (m, 2H, *m*-Mes), 6.46 (d, $^3J_{HH}$ = 2.8 Hz, 1H, C*H*-backbone), 6.04 (d, $^3J_{HH}$ = 2.7 Hz, 1H, C*H*-backbone), 2.25 (s, 3H, *p*-CH_3), 2.18 (br. d, $^3J_{HH}$ = 2.5 Hz, 6H, CH_2-Ad), 2.09 (s, 9H, *o*-CH_3 + C*H*-Ad), 1.80–1.58 (br. m, 6H, CH_2-Ad).

^{13}C NMR (126 MHz, $CDCl_3$): δ = 141.9 (s, N*C*N), 137.8 (s, *p*-Mes), 136.6 (s, *o*-Mes), 132.7 (s, i-Mes), 128.7 (s, *m*-Mes), 112.4 (s, *C*H-backbone), 108.6 (s, *C*H-backbone), 57.8 (s, *C*q-Ad), 39.9 (s, *C*H_2-Ad), 35.8 (s, *C*H_2-Ad), 29.7 (s, *C*H-Ad), 21.1 (s, *p*-*C*H_3), 17.9 (s, *o*-*C*H_3).

EA (%) calc. for $C_{44}H_{56}Cl_2N_6Ti$ (788 g mol^{-1}): C 67.09, H 7.17, N 10.67; found: C 67.06, H 7.535, N 10.30.

[(Im^{AdDipp}N)$_2$TiCl$_2$] (6b). A solution of imine **2b** (500 mg, 1.11 mmol, 2 eq.) in 30 mL toluene was added to a solution of [$TiCl_4(THF)_2$] (185 mg, 0.56 mmol, 1 eq.) in 10 mL toluene. The yellow reaction mixture was stirred for 16 h at 100 °C upon which a color change to orange could be observed. The solvent was removed under high vacuum and the residue was crystallised from CH_2Cl_2/*n*-hexane. The crystals were washed several times with small amounts of *n*-hexane and subsequent removal of all volatiles under high vacuum yielded product **6b** as an orange crystalline powder (387 mg, 0.44 mmol, 79%).

^{1}H NMR (500 MHz, $CDCl_3$): δ = 7.31–7.25 (m, 1H, *p*-Dipp), 7.18–7.14 (m, 2H, *m*-Dipp), 6.45 (d, $^3J_{HH}$ = 2.7 Hz, 1H, C*H*-backbone), 6.14 (d, $^3J_{HH}$ = 2.7 Hz, 1H, C*H*-backbone), 2.78 (sept, $^3J_{HH}$ = 6.9 Hz, 2H, C*H*(CH_3)$_2$), 2.16 (br. s, 6H, CH_2-Ad), 2.09 (br. s, 3H, C*H*-Ad), 1.82–1.57 (br. m, 6H, CH_2-Ad), 1.33 (d, $^3J_{HH}$ = 7.0 Hz, 6H, CH(CH_3)$_2$), 1.02 (d, $^3J_{HH}$ = 6.9 Hz, 6H, CH(CH_3)$_2$).

^{13}C NMR (126 MHz, $CDCl_3$): δ = 147.0 (s, *o*-Dipp), 142.5 (s, N*C*N), 133.0 (s, i-Dipp), 129.1 (s, *p*-Dipp), 123.7 (s, *m*-Dipp), 114.3 (s, *C*H-backbone), 108.2 (s, *C*H-backbone), 58.4 (s, *C*q-Ad), 40.3 (s, *C*H_2-Ad), 35.9 (s, *C*H_2-Ad), 29.9 (s, *C*H-Ad), 28.8 (s, *C*H(CH_3)$_2$), 25.4 (s, CH(CH_3)$_2$), 23.2 (s, CH(CH_3)$_2$).

EA (%) calc. for $C_{50}H_{68}Cl_2N_6Ti{\cdot}0.5$ (CH_2Cl_2) (872 g mol^{-1}): C 66.34, H 7.61, N 9.19, found: C 66.84, H 7.703, N 8.91.

Conflicts of interest

There are no conflicts to declare.

Acknowledgements

M. T. and M. E. thank the German Israel Foundation (GIF) for continuous support in the years 2010–2012 and 2015–2017.

Notes and references

1 (*a*) N. Kuhn, R. Fawzi, M. Steimann, J. Wiethoff, D. Bläser and R. Boese, *Z. Naturforsch., B: J. Chem. Sci.*, 1995, **50**, 1779–1784; (*b*) N. Kuhn, M. Göhner, M. Grathwohl, J. Wiethoff, G. Frenking and Y. Chen, *Z. Anorg. Allg. Chem.*, 2003, **629**, 793–802.

2 N. Kuhn, R. Fawzi, M. Steimann and J. Wiethoff, *Z. Anorg. Allg. Chem.*, 1997, **623**, 769–774.

3 M. Tamm, S. Randoll, T. Bannenberg and E. Herdtweck, *Chem. Commun.*, 2004, 876–877.

4 M. Tamm, S. Randoll, E. Herdtweck, N. Kleigrewe, G. Kehr, G. Erker and B. Rieger, *Dalton Trans.*, 2006, 459–467.

5 M. Tamm, D. Petrovic, S. Randoll, S. Beer, T. Bannenberg, P. G. Jones and J. Grunenberg, *Org. Biomol. Chem.*, 2007, **5**, 523–530.

6 (*a*) X. Wu and M. Tamm, *Coord. Chem. Rev.*, 2014, **260**, 116–138; (*b*) A. Doddi, M. Peters and M. Tamm, *Chem. Rev.*, 2019, **119**, 6994–7112; (*c*) P. Raja, S. Revathi and T. Ghatak, *Eng. Sci.*, 2020, **12**, 23–37.

7 (*a*) S. H. Stelzig, M. Tamm and R. M. Waymouth, *J. Polym. Sci., Part A: Polym. Chem.*, 2008, **46**, 6064–6070; (*b*) K. Nomura, H. Fukuda, W. Apisuk, A. G. Trambitas, B. Kitiyanan and M. Tamm, *J. Mol. Catal. A: Chem.*, 2012, **363–364**, 501–511; (*c*) W. Apisuk, A. G. Trambitas, B. Kitiyanan, M. Tamm and K. Nomura, *J. Polym. Sci., Part A: Polym. Chem.*, 2013, **51**, 2575–2580.

8 M. Sharma, H. S. Yameen, B. Tumanskii, S.-A. Filimon, M. Tamm and M. S. Eisen, *J. Am. Chem. Soc.*, 2012, **134**, 17234–17244.

9 D. Shoken, M. Sharma, M. Botoshansky, M. Tamm and M. S. Eisen, *J. Am. Chem. Soc.*, 2013, **135**, 12592–12595.

10 (*a*) D. Shoken, L. J. W. Shimon, M. Tamm and M. S. Eisen, *Organometallics*, 2016, **35**, 1125–1131; (*b*) K. Naktode, S. Das, H. P. Nayek and T. K. Panda, *Inorg. Chim. Acta*, 2017, **456**, 24–33.

11 S. Das, J. Bhattacharjee and T. K. Panda, *Dalton Trans.*, 2019, **48**, 7227–7235.

12 (*a*) K. Naktode, S. Das, H. P. Nayek and T. K. Panda, *J. Coord. Chem.*, 2018, **71**, 4148–4163; (*b*) K. Naktode, S. Das, J. Bhattacharjee, H. P. Nayek and T. K. Panda, *Inorg. Chem.*, 2016, **55**, 1142–1153.

13 (*a*) J. R. Aguilar-Calderón, A. J. Metta-Magaña, B. Noll and S. Fortier, *Angew. Chem., Int. Ed.*, 2016, **55**, 14101–14105; (*b*) J. R. Aguilar-Calderón, J. Murillo, A. Gomez-Torres, C. Saucedo, A. Jordan, A. J. Metta-Magaña, M. Pink and S. Fortier, *Organometallics*, 2020, **39**, 295–311.

14 (*a*) W. P. Kretschmer, C. Dijkhuis, A. Meetsma, B. Hessen and J. H. Teuben, *Chem. Commun.*, 2002, 608–609; (*b*) K. Nomura, H. Fukuda, S. Katao, M. Fujiki, H. J. Kim, D.-H. Kim and S. Zhang, *Dalton Trans.*, 2011, **40**, 7842–7849; (*c*) I. Haas, C. Hübner, W. P. Kretschmer and R. Kempe, *Chem. – Eur. J.*, 2013, **19**, 9132–9136; (*d*) K. Nomura, S. Patamma, H. Matsuda, S. Katao, K. Tsutsumi and H. Fukuda, *RSC Adv.*, 2015, **5**, 64503–64513; (*e*) K. Nomura, H. Fukuda, H. Matsuda, S. Katao and S. Patamma, *J. Organomet. Chem.*, 2015, **798**, 375–383; (*f*) Z.-Q. Zhang, J.-T. Qu, S. Zhang, Q.-P. Miao and Y.-X. Wu, *Polym. Chem.*, 2018, **9**, 48–59; (*g*) T. Dietel, F. Lukas, W. P. Kretschmer and R. Kempe, *Science*, 2022, **375**, 1021–1024.

15 (*a*) A. Glöckner, T. Bannenberg, C. G. Daniliuc, P. G. Jones and M. Tamm, *Inorg. Chem.*, 2012, **51**, 4368–4378; (*b*) J. Klosin, P. P. Fontaine, R. Figueroa, S. D. McCann and D. Mort, *Organometallics*, 2013, **32**, 6488–6499; (*c*) M. Khononov, N. Fridman, M. Tamm and M. S. Eisen, *Eur. J. Org. Chem.*, 2020, 3153–3160.

16 (*a*) S. Zhang, M. Tamm and K. Nomura, *Organometallics*, 2011, **30**, 2712–2720; (*b*) K. Nomura, B. K. Bahuleyan, K. Tsutsumi and A. Igarashi, *Organometallics*, 2014, **33**, 6682–6691; (*c*) K. Nomura, B. K. Bahuleyan, S. Zhang, P. M. V. Sharma, S. Katao, A. Igarashi, A. Inagaki and M. Tamm, *Inorg. Chem.*, 2014, **53**, 607–623.

17 (*a*) S. Beer, C. G. Hrib, P. G. Jones, K. Brandhorst, J. Grunenberg and M. Tamm, *Angew. Chem., Int. Ed.*, 2007, **46**, 8890–8894; (*b*) S. Beer, K. Brandhorst, J. Grunenberg, C. G. Hrib, P. G. Jones and M. Tamm, *Org. Lett.*, 2008, **10**, 981–984; (*c*) B. Haberlag, X. Wu, K. Brandhorst, J. Grunenberg, C. G. Daniliuc, P. G. Jones and M. Tamm, *Chem. – Eur. J.*, 2010, **16**, 8868–8877; (*d*) B. Haberlag, M. Freytag, C. G. Daniliuc, P. G. Jones and M. Tamm, *Angew. Chem., Int. Ed.*, 2012, **51**, 13019–13022; (*e*) S. Lysenko, C. G. Daniliuc, P. G. Jones and M. Tamm, *J. Organomet. Chem.*, 2013, **744**, 7–14; (*f*) B. Haberlag, M. Freytag, P. G. Jones and M. Tamm, *Adv. Synth. Catal.*, 2014, **356**, 1255–1265; (*g*) Z. S. Qureshi, A. Hamieh,

S. Barman, N. Maity, M. K. Samantaray, S. Ould-Chikh, E. Abou-Hamad, L. Falivene, V. D'Elia, A. Rothenberger, I. Llorens, J.-L. Hazemann and J.-M. Basset, *Inorg. Chem.*, 2017, **56**, 861–871.

18 (*a*) T. K. Panda, S. Randoll, C. G. Hrib, P. G. Jones, T. Bannenberg and M. Tamm, *Chem. Commun.*, 2007, 5007–5009; (*b*) A. G. Trambitas, J. Yang, D. Melcher, C. G. Daniliuc, P. G. Jones, Z. Xie and M. Tamm, *Organometallics*, 2011, **30**, 1122–1129.

19 A. G. Trambitas, T. K. Panda and M. Tamm, *Z. Anorg. Allg. Chem.*, 2010, **636**, 2156–2171.

20 T. K. Panda, A. G. Trambitas, T. Bannenberg, C. G. Hrib, S. Randoll, P. G. Jones and M. Tamm, *Inorg. Chem.*, 2009, **48**, 5462–5472.

21 (*a*) A. G. Trambitas, T. K. Panda, J. Jenter, P. W. Roesky, C. Daniliuc, C. G. Hrib, P. G. Jones and M. Tamm, *Inorg. Chem.*, 2010, **49**, 2435–2446; (*b*) A. G. Trambitas, D. Melcher, L. Hartenstein, P. W. Roesky, C. Daniliuc, P. G. Jones and M. Tamm, *Inorg. Chem.*, 2012, **51**, 6753–6761.

22 B.-C. Liu, N. Ge, Y.-Q. Zhai, T. Zhang, Y.-S. Ding and Y.-Z. Zheng, *Chem. Commun.*, 2019, **55**, 9355–9358.

23 S. Revathi, P. Raja, S. Saha, M. S. Eisen and T. Ghatak, *Chem. Commun.*, 2021, **57**, 5483–5502.

24 (*a*) I. S. R. Karmel, N. Fridman, M. Tamm and M. S. Eisen, *J. Am. Chem. Soc.*, 2014, **136**, 17180–17192; (*b*) I. S. R. Karmel, M. Botoshansky, M. Tamm and M. S. Eisen, *Inorg. Chem.*, 2014, **53**, 694–696; (*c*) I. S. R. Karmel, N. Fridman, M. Tamm and M. S. Eisen, *Organometallics*, 2015, **34**, 2933–2942; (*d*) I. S. R. Karmel, M. Khononov, M. Tamm and M. S. Eisen, *Catal. Sci. Technol.*, 2015, **5**, 5110–5119; (*e*) I. S. R. Karmel, M. Tamm and M. S. Eisen, *Angew. Chem., Int. Ed.*, 2015, **54**, 12422–12425.

25 M. Yadav, A. Metta-Magaña and S. Fortier, *Chem. Sci.*, 2020, **11**, 2381–2387.

26 (*a*) J. T. Goettel, H. Gao, S. Dotzauer and H. Braunschweig, *Chem. – Eur. J.*, 2020, **26**, 1136–1143; (*b*) T. Glöge, F. Aal, S.-A. Filimon, P. G. Jones, J. Michaelis de Vasconcellos, S. Herres-Pawlis and M. Tamm, *Z. Anorg. Allg. Chem.*, 2015, **641**, 2204–2214.

27 (*a*) W. Zhao, B. Wang, B. Dong, H. Liu, Y. Hu, M. S. Eisen and X. Zhang, *Organometallics*, 2020, **39**, 3983–3991; (*b*) H. Liu, M. Khononov, N. Fridman, M. Tamm and M. S. Eisen, *Inorg. Chem.*, 2017, **56**, 3153–3157; (*c*) H. Liu, N. Fridman, M. Tamm and M. S. Eisen, *Organometallics*, 2017, **36**, 4600–4610; (*d*) H. Liu, N. Fridman, M. Tamm and M. S. Eisen, *Organometallics*, 2017, **36**, 3896–3903; (*e*) H. Liu, M. Khononov, N. Fridman, M. Tamm and M. S. Eisen, *J. Organomet. Chem.*, 2018, **857**, 123–137; (*f*) H. Liu, K. Kulbitski, M. Tamm and M. S. Eisen, *Chem. – Eur. J.*, 2018, **24**, 5738–5742; (*g*) H. Liu, M. Khononov, N. Fridman, M. Tamm and M. S. Eisen, *Inorg. Chem.*, 2019, **58**, 13426–13439; (*h*) M. Khononov, H. Liu, N. Fridman, M. Tamm and M. S. Eisen, *Organometallics*, 2020, **39**, 3021–3033.

28 P. Queval, C. Jahier, M. Rouen, I. Artur, J.-C. Legeay, L. Falivene, L. Toupet, C. Crévisy, L. Cavallo, O. Baslé and M. Mauduit, *Angew. Chem., Int. Ed.*, 2013, **52**, 14103–14107.

29 R. Tarrieu, A. Dumas, J. Thongpaen, T. Vives, T. Roisnel, V. Dorcet, C. Crévisy, O. Baslé and M. Mauduit, *J. Org. Chem.*, 2017, **82**, 1880–1887.

30 (*a*) A. Dumas, R. Tarrieu, T. Vives, T. Roisnel, V. Dorcet, O. Baslé and M. Mauduit, *ACS Catal.*, 2018, **8**, 3257–3262; (*b*) J. Morvan, T. McBride, I. Curbet, S. Colombel-Rouen, T. Roisnel, C. Crévisy, D. L. Browne and M. Mauduit, *Angew. Chem., Int. Ed.*, 2021, **60**, 19685–19690.

31 (*a*) F. H. Allen, O. Kennard, D. G. Watson, L. Brammer, A. G. Orpen and R. Taylor, *J. Chem. Soc., Perkin Trans. 2*, 1987, S1; (*b*) J. March, *Advanced Organic Chemistry*, John Wiley & Sons, Inc, New York, 4th edn, 1992.

32 C. Camp, L. C. E. Naested, K. Severin and J. Arnold, *Polyhedron*, 2016, **103**, 157–163.

33 H. H. Brintzinger, D. Fischer, R. Mülhaupt, B. Rieger and R. M. Waymouth, *Angew. Chem., Int. Ed. Engl.*, 1995, **34**, 1143–1170.

34 T. Ochiai, D. Franz and S. Inoue, *Chem. Soc. Rev.*, 2016, **45**, 6327–6344.

35 W. L. F. Armarego and C. L. L. Chai, *Purification of laboratory chemicals*, Elsevier/Butterworth-Heinemann, Amsterdam, London, 7th edn, 2013.

36 G. R. Fulmer, A. J. M. Miller, N. H. Sherden, H. E. Gottlieb, A. Nudelman, B. M. Stoltz, J. E. Bercaw and K. I. Goldberg, *Organometallics*, 2010, **29**, 2176–2179.